Bioresource Technology 166 (2014) 235–242

Contents lists available at ScienceDirect

Bioresource Technology

journal homepage: www.elsevier.com/locate/biortech

Biocatalytic and antimicrobial activities of gold nanoparticles synthesized by *Trichoderma* sp.

Aradhana Mishra [a], Madhuree Kumari [a], Shipra Pandey [a], Vasvi Chaudhry [a], K.C. Gupta [b], C.S. Nautiyal [a,*]

[a] Division of Plant Microbe Interactions, CSIR-National Botanical Research Institute, Rana Pratap Marg, Lucknow 226001, India
[b] CSIR-Indian Institute of Toxicology Research, 80, Mahatma Gandhi Marg, Qaiserbagh, Lucknow 226001, India

HIGHLIGHTS

- A clean, rapid, and ecofriendly method of nanoparticles biosynthesis was developed.
- Method used *Trichoderma viride* and *Hypocrea lixii* for nanoparticles biosynthesis.
- The method reports use of non-pathogenic fungi in rapid synthesis of gold nanoparticle for the first time.
- Nanoparticles displayed antimicrobial potential and biocatalytic properties.
- The method altered nanoparticles for desired size and geometry.

GRAPHICAL ABSTRACT

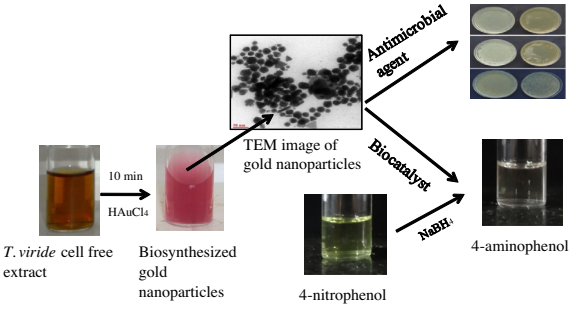

ARTICLE INFO

Article history:
Received 11 March 2014
Received in revised form 21 April 2014
Accepted 23 April 2014
Available online 9 May 2014

Keywords:
Gold nanoparticles
Biosynthesis
Trichoderma viride
Hypocrea lixii
Biocatalyst

ABSTRACT

The aim of this work was to synthesize gold nanoparticles by *Trichoderma viride* and *Hypocrea lixii*. The biosynthesis of the nanoparticles was very rapid and took 10 min at 30 °C when cell-free extract of the *T. viride* was used, which was similar by *H. lixii* but at 100 °C. Biomolecules present in cell free extracts of both fungi were capable to synthesize and stabilize the formed particles. Synthesis procedure was very quick and environment friendly which did not require subsequent processing. The biosynthesized nanoparticles served as an efficient biocatalyst which reduced 4-nitrophenol to 4-aminophenol in the presence of $NaBH_4$ and had antimicrobial activity against pathogenic bacteria. To the best of our knowledge, this is the first report of such rapid biosynthesis of gold nanoparticles within 10 min by *Trichoderma* having plant growth promoting and plant pathogen control abilities, which served both, as an efficient biocatalyst, and a potent antimicrobial agent.

1. Introduction

Nanotechnology has revolutionized every aspect of human life. Ranging from medicine to cosmetics, agriculture, and food safety to pollution detection and their bioremediation, electronics to energy, every facet of life has been recolored with nanotechnology (Kuang et al., 2013). They exhibit a complete range of new and improved characteristics over the bulk material from which they have been synthesized. The strong correlation between size and properties of nanoparticles offer innumerable opportunities for brilliant discoveries. The often unexpected behaviors of nanoparticles possess a great potential for innovative technology and their application for human welfare (Heiligtag and Niederberger, 2013; Mullai et al., 2013).

Metal nanoparticles such as gold, silver, and platinum show an array of applications (Knöpfel and Akemann, 2010). Among the metal nanoparticles, gold nanoparticles have received enormous attention because of their wide range of applications in biology, catalysis, optics, and many more (Heiligtag and Niederberger,

* Corresponding author. Tel./fax: +91 522 2206651.
E-mail address: nautiyalnbri@lycos.com (C.S. Nautiyal).

http://dx.doi.org/10.1016/j.biortech.2014.04.085
0960-8524/

2013). Although gold is one of the most ancient subjects of curiosity, its renaissance in nanotechnology has led to an exceptional increase in its applications. Though several chemical and physical approaches are available for synthesis of gold nanoparticles, focus has now been shifted toward greener approach because of ease of biosynthesis and elimination of harsh chemical procedures (Das et al., 2012). Several plants, fungal, bacterial, actinomycetes and agro waste (Gan et al., 2012) have the potential to biosynthesize nanoparticles (Kaushik et al., 2010). Fungi are considered a better source for higher productivity of nanoparticles because of the proteins (Du et al., 2011) and secondary metabolites secreted extracellularly. The extracellular synthesis of nanoparticles has attracted more attention due to its simplicity, no further downstream processing and lesser time consumption in comparison to intracellular synthesis during the reaction. The size and shape of the nanoparticles synthesized extracellularly can also be manipulated by controlling growth parameters such as pH, temperature, substrate concentration and reaction time (Sathishkumar et al., 2010).

A major drawback with green synthesis of nanoparticles is the reaction time which can range to several days as compared with chemical and physical synthesis which takes minutes or hours. There are few reports available which shows the rapid synthesis of nanoparticles in short span of time. Reports on rapid synthesis of silver nanoparticles within 5 min using culture supernatant of Enterobacteria is available (Shahverdi et al., 2007). Similarly, biosynthesis of gold nanoparticles within a minute with supernatant of *Penicillium* has also been reported (Du et al., 2011). The drawbacks of above reports are that microbes involved in rapid synthesis are well known as pathogens which may cause serious problem during their further applications. To avoid these complications, *Trichoderma* a plant growth promoter and biocontrol agent was selected for biosynthesis of gold nanoparticles. *Trichoderma* sp. are telomorph bearing filamentous fungi, plant symbionts which can colonize the apoplast of plant roots. They are well known for their plant growth promoting, pathogen control and bioremediation potential abilities (Mishra and Nautiyal, 2009; Tripathi et al., 2013).

Gold nanoparticles have attracted significant scientific interest as a new generation of antimicrobial agents because of increasing resistance of bacteria toward antibiotics. Their capability to produce cellular damage by various means make it very difficult for bacteria to acquire resistance against them (Cui et al., 2012).

There is an urgent need to develop green sustainable technologies which can bioremediate organic pollutants efficiently. Normally, it takes very long time to degrade organic compounds such as 4-nitrophenol which may threaten the aquatic life. To cop up with these problems, the development of highly selective reaction systems using heterogeneous catalysts is greatly desired (Ai and Jiang, 2013). Gold nanoparticles fulfill the criteria to act as a heterogeneous catalyst to bring about the conversion of 4-nitrophenol to 4-aminophenol quickly in presence of $NaBH_4$.

In this study, we report the rapid biosynthesis of gold nanoparticles within a minute with cell free extract of *Trichoderma viride* and recombinant *Hypocrea lixii* at different reaction temperatures. To the best of our knowledge, this is the first report of rapid synthesis of gold nanoparticles by *Trichoderma* sp. which can act as an antimicrobial agent, as well as, an efficient biocatalyst.

2. Methods

2.1. Chemicals

The Gold (III) chloride (ACS reagent) was purchased from Sigma Aldrich. All other reagents used were of Analytical grade.

2.2. Biocontrol activity

The culture filtrates of *T. viride* and *H. lixii* were assayed for their biocontrol potential by plate assay method (Kumar et al., 2012). Sterilized cell free extract of seven day old *Trichoderma* cultures were used to estimate biocontrol activity against *Fusarium oxysporum*. Five milliliters of filtrate was mixed with 20 ml of Potato Dextrose Agar (PDA) and poured in Petri plates while control plates were prepared by addition of 5 ml of MQ water with 20 ml of PDA. A bid of *F. oxysporum* was placed on the center of the above prepared plates. Percent inhibition of *F. oxysporum* was calculated by comparing them with control plate (without bid of *F. oxysporum*), after seven days of inoculation.

2.3. Fungal cell free extract preparation and synthesis of gold nanoparticles

Fungal strains *T. viride* (MTCC 5661) and *H. lixii* (MTCC 5659) were used for biosynthesis of gold nanoparticles. To prepare cell free extract, fungi were grown in 100 ml of Potato Dextrose Broth for 4 days at 28 °C and agitated at 80 rpm. After 4 days, the biomass obtained was filtered from Whatman filter paper No. 1 and washed with autoclaved MQ water 3 times. The filtered and washed biomass was resuspended in 100 ml of sterile deionized water for 3 days. The cell free extracts were obtained by filtering out the biomass. To check the effect of various biological parameters, the reaction was carried out at 20 °C, 30 °C, 40 °C, 50 °C, and 100 °C of temperature and pH was varied at 5, 7, and 9. Three different concentrations of cell free extract (10%, 50%, and 100%) and two different concentrations of $HAuCl_4$ (250 and 500 mg/l) were assessed for rapid synthesis of gold nanoparticles. To check the rapid biosynthesis, reaction was carried out at various time intervals of 1, 2, 3, 5, 10, and 15 min.

2.4. Characterization of gold nanoparticles

Preliminary characterization of gold nanoparticles was done through visual observation for change in color of cell free extract. Further the reduction studies of gold ions to gold nanoparticles were done through UV–vis spectroscopy (Thermo Specrtascan UV 2700) (Ahmad et al., 2003). For the kinetics study, UV–vis spectra was recorded for 5 min at an interval of 30 s. Further, to study the hydrodynamic size and poly dispersity index (PDI) of the nanoparticles biosynthesized, particle size analyzer was used (Malvern, nanoseries zeta sizer) (Sujitha and Kannan, 2013). To investigate the particle size and morphology, transmission electron microscopy (TEM) was carried out (Ahmad et al., 2003). Samples were filtered through 0.45 μ syringe Millipore filters and sonicated for 2 min. After sonication, a drop of solution was placed immediately on foamwar coated copper grid and left overnight for drying. Bright field TEM studies were carried out using at 80 kV. Selected Area Electron Diffraction (SAED) pattern was also recorded to find the crystalline nature of biosynthesized nanoparticles. Energy Dispersive X-ray Analysis (EDAX) spectrums of the rapidly synthesized gold nanoparticles were carried out on a scanning electron microscopy (Du et al., 2011). The samples were freeze dried and casted on a glass substrate. The electron backscatter diffraction was used during the analysis, and the EDS aperture was set to 60 μm and operated at 20 kV.

2.5. Antimicrobial activity of gold nanoparticles

2.5.1. Broth and plate assay

To assess the antimicrobial potential of gold nanoparticles, three pathogenic bacteria *Pseudomonas syringae*, *Escherichia coli*, and *Shigella sonnei* were selected. Plates of nutrient agar and Luria

agar were prepared supplemented with 5%, 10%, 20%, and 25% of biogenic gold nanoparticles synthesized by *T. viride* cell free extract and their antimicrobial activity was visualized. The control plates were prepared without biogenic gold nanoparticles in medium. For quantitative studies, 100 ml of nutrient broth and Luria broth were mixed with 5%, 10%, 20%, and 25% of biogenic gold nanoparticles and broth without gold nanoparticles served as control. 1% of overnight grown cultures were inoculated and their colony forming units were counted at different time intervals of 1st, 2nd, 3rd, 5th and 7th day.

2.5.2. Immobilization of gold nanoparticles on cloth and disk diffusion studies

Immobilization of gold nanoparticles on cloth and disk diffusion studies were carried out following the method of Sathishkumar et al. (2010) with some modifications. Desired amount of nanoparticles were suspended in 5 ml of sterile distilled water and 5 ml of Poly Vinyl Pyrrolidone (PVP). 100 µl of overnight grown culture of *S. sonnei* was applied uniformly on nutrient agar plates. Presterilized cotton cloth of 1 cm^2 was placed on the center of the plates and pipetted with 50, 75, and 100 µl of gold nanoparticles and allowed to air dry. The plates were incubated at 28 °C for 24 h, after which the zone of inhibition was observed.

2.6. Catalytic activity of gold nanoparticles in 4-nitrophenol degradation

Catalytic activities of biosynthesized gold nanoparticles were studied as described by Gangula et al. (2011) with some modifications. To 1.7 ml of water, 0.3 ml of 2 mM solution of 4-nitrophenol, and 1 ml of 0.03 M of freshly prepared $NaBH_4$ solution were mixed in a 3 ml standard quartz cuvette (path length 1 cm). To this reaction mixture, 50 µl of biogenic gold nanoparticles were added. The 4-nitrophenol shows an absorbance peak at 400 nm in presence of $NaBH_4$, so the progress of the reaction was monitored by tracking the decrease in the absorption spectra of 4-nitrophenolate ion at 400 nm and increase in absorbance at 260 nm due formation of 4-aminophenol. Kinetics of the reaction was monitored for a time period of 45 min for decrease in absorbance at 400 nm and increase in absorbance at 260 nm at a time interval of 2 min.

3. Results and discussion

3.1. Isolation and Identification of fungal isolates

Two fungal isolates *T. viride* (MTCC 5661) and *H. lixii* (MTCC 5659) were selected for green synthesis of nanoparticles. MTCC 5661 was isolated from CSIR-NBRI Garden Campus and the second recombinant fungal isolate MTCC 5659 was a result of protoplast fusion between *T. viride* and *H. lixii* (MTCC 5660). The isolates were identified by morphological, biochemical and ITS sequence analysis and deposited in Microbial Type Culture Collection (MTCC), Chandigarh, India.

3.2. Biocontrol activity of T. viride and H. lixii

Both *Trichoderma* isolates were found to be potent biocontrol agents against *F. oxysporum*. With *T. viride*, the inhibition was found to be 42.12% while *H. lixii* controlled the pathogen to 35.18%. The result clearly demonstrates the presence of secondary metabolites in cell free extract of *Trichoderma* which had the potential to control plant pathogens. The results are in accordance with previous studies of Kumar et al. (2012).

3.3. Extracellular biosynthesis of gold nanoparticles

3.3.1. Effect of reaction temperature and incubation time of T. viride

Observations were taken under different temperatures (20 °C, 30 °C, 40 °C and 50 °C) during reaction where change in color of cell free extract of *T. viride* was found within 10 min of time interval only at 30 °C. The same experiment with cell free extract of *H. lixii* was not showing any quick biosynthesis of gold nanoparticles, under different reaction temperatures, indicating the potential of gold nanoparticles formation in such short interval of time was isolate and temperature specific. Among several isolates evaluated, only *T. viride* was able to biosynthesize gold nanoparticles at 30 °C. Few reports are available for biosynthesis of gold nanoparticles from isolates of *Trichoderma* (Mukherjee et al., 2012) however to the best of our knowledge, this the first report of rapid biosynthesis of gold nanoparticles within minutes by *Trichoderma* sp.

Reduction of gold ions to gold nanoparticles when exposed to the cell free extract of *T. viride* and *H. lixii* was checked visually by change in color of the solution and reaction kinetics was monitored using UV–vis spectroscopy. The color of cell free extract of *T. viride* started to change from pale yellow to brown within a minute of addition of $HAuCl_4$, which turned into pink after 10 min of incubation at 30 °C where as the color of control remained the same throughout the incubation period (Fig. S1a and b). The change in color of the solution was due to the excitation of surface plasmon vibrations in the gold nanoparticles, a characteristic property of the synthesized nanoparticles (Song et al., 2009).

To further confirm the results, UV–vis spectra of culture extract of *T. viride* was recorded within 15 min of incubation with 250 mg/l of $HAuCl_4$ at 30 °C (Fig. S1c). Cell free extract without addition of $HAuCl_4$ did not show any peak absorbance in the range of 500–600 nm, while the absorption peak was recorded at 528 nm after 1 min by addition of $HAuCl_4$ to cell free extract of *T. viride*. Gold nanoparticles are known to exhibit an absorption peak between 500 and 600 nm due to excitation of the surface plasmon vibrations in the gold nanoparticles (Song et al., 2009; Du et al., 2011). Previous reports have also proved that the resonance peak of gold nanoparticles appears around this region, but the exact position depends on a number of factors (Eustisa and El-Sayed, 2006). The maximum absorption peak shifted to 520 nm after 2 min from 528 nm due to further reduction in size of gold nanoparticles (Abdelhalim et al., 2012) lasting up to 5 min. The maximum extinction of Surface Plasmon Band (SPB) further increased to 540 nm and remained stable thereafter. The shift may be due to aggregation of smaller particles to form the bigger ones. The surface Plasmon resonance band of the gold particles is red shifted with the increase in particle size in accordance with Mie theory (Haiss et al., 2007).

The broader Surface Plasmon Band (SPB) also suggests the anisotropy of the particles. Initially, up to 5 min, the gold nanoparticles showed broader bandwidth of maximal surface Plasmon resonance due to anisotropic nature of the particles. The broad SPB at lower quantities of the extract due to the formation of large anisotropic particles with *Citrus limon* is also reported (Sujitha and Kannan, 2013). With increase in time, the broadening of the peak decreased with a red shift indicating the increase in particle size and decrease in anisotropy.

3.3.2. Reaction kinetics

To monitor the reaction kinetics, a fixed wavelength i.e. 540 nm was selected because the maximum absorbance (1.568) was observed at this wavelength. From the results, it was observed that the absorbance increased rapidly during the first 30 s after the addition of $HAuCl_4$, indicating the rapid biosynthesis of gold nanoparticles.

Further, when the reaction mixture was boiled at 100 °C, the color again started to change to brown within fraction of seconds and turned into pink within 5 min of boiling. The maximum absorption reached to 0.98 at 532 nm, much earlier than the nanoparticles biosynthesized at room temperature.

3.3.3. Effect of reaction temperature and incubation time of H. lixii

The cell free extract of *H. lixii* also showed the similar results. After boiling the extract at 100 °C, the color changed immediately to brown and then to pink and a Surface Plasmon Band was observed at 530 nm after 5 min of boiling. Though the maximum absorbance increased to 1.098 from 0.650 after boiling till 30 min, no alteration was found in SPB indicating the stability of particles synthesized. It gives a clear picture about the nanotizing efficacy of *H. lixii* that there is no change in formation of nanoparticles in both time duration, though the rate of biosynthesis increased with increase in time. Earlier reports had also suggested that with an increase in reaction temperature, rate of nanoparticles synthesis also increased. Increasing the reaction temperature, during reduction of $HAuCl_4$ with cell free extract of *Trichoderma* sp. results in an increase in the rate of reduction of gold ions, which leads to an enhanced nucleation rate and an enhanced synthesis of nanoparticles (Song et al., 2009). The result suggests that for such rapid extracellular biosynthesis, either, there is involvement of secondary metabolites or proteins present in supernatant of *T. viride* and *H. lixii* in biosynthesizing gold nanoparticles, even after denaturation. Though several researchers have emphasized on the role of protein and secondary metabolites for transformation of gold salt into colloidal gold solution (Ahmad et al., 2003), the exact mechanism of biosynthesis of nanoparticles remains unknown.

3.3.4. Hydrodynamic diameter and poly dispersity index (PDI)

To observe the particle size and mono/poly dispersity of gold nanoparticles synthesized by *T. viride* and *H. lixii*, particles were characterized through zeta sizer. Fig. 1 shows the *Z* value of biosynthesized gold nanoparticles within a time span of 15 min at 30 °C by *T. viride* and their respective PDI. The hydrodynamic size also confirms the rapid synthesis of gold nanoparticles. The size reduced to 95 nm within a minute after addition of $HAuCl_4$ to *T. viride* supernatant. In agreement with the results obtained with UV–vis spectroscopy, the hydrodynamic diameter further reduced to 69 nm after completion of 5 min of the reaction. The diameter further decreased to 61 nm after 10 min of incubation. No further decrease in hydrodynamic diameter was observed after further incubation of the reaction mixture.

The dynamic light scattering (DLS) instrument is known to measure the shell thickness of a capping or stabilizing agent enveloping the metallic particles along with the actual size of the metallic core (Sujitha and Kannan, 2013). The size observed in DLS measurement is generally larger than the size observed in transmission electron microscopy (TEM) because the measured size also includes the bio-organic compounds enveloping the core of the AuNPs (Kasthuri et al., 2009). Though the observed size in DLS measurement is larger than the actual size, the results best fitted in the category to be considered as nanoparticles biosynthesized quickly within a minute, again indicating the potential of *T. viride* supernatant to synthesize gold nanoparticles very rapidly.

Fig. 1 shows the PDI of biosynthesized gold nanoparticles within 15 min of reaction time at 30 °C. PDI value represents the relative variance in the particle size distribution, the more monodisperse the particles, the lower the PDI (Tanga et al., 2009). It clearly indicates the polydispersity of the gold nanoparticles. The PDI value decreased from 0.383 at 1 min to 0.309 after 2 min. It may be due to reduction of gold nanoparticles size and increase in monodispersity to spherical shape. After boiling the reaction mixture for 5 min, the hydrodynamic diameter reduced to 59 nm and did not show any major variations till 30 min of boiling (Fig. 2). The consistency in the size can be explained on the phenomenon that at higher temperature, most of the gold ions form nuclei but their secondary growth seized because of higher reaction temperature (Burda et al., 2005). The higher PDI value indicated the polydiverse nature of nanoparticles.

Similarly, cell free extract of *H. lixii* showed a hydrodynamic diameter of 60 nm and did not show any further variations in accordance with the UV–vis spectroscopy (Fig. 3). The results obtained with *T. viride* and *H. lixii* were quite similar indicating the role of similar mechanism involved in biosynthesis of gold nanoparticles at 100 °C but *T. viride* and *H. lixii* showed different pattern in PDI quantification. PDI index of *H. lixii* decreased from 0.5 to 0.3 indicated the decrease in polydispersity as the time interval of boiling increased, whereas the PDI of *T. viride* remained constant.

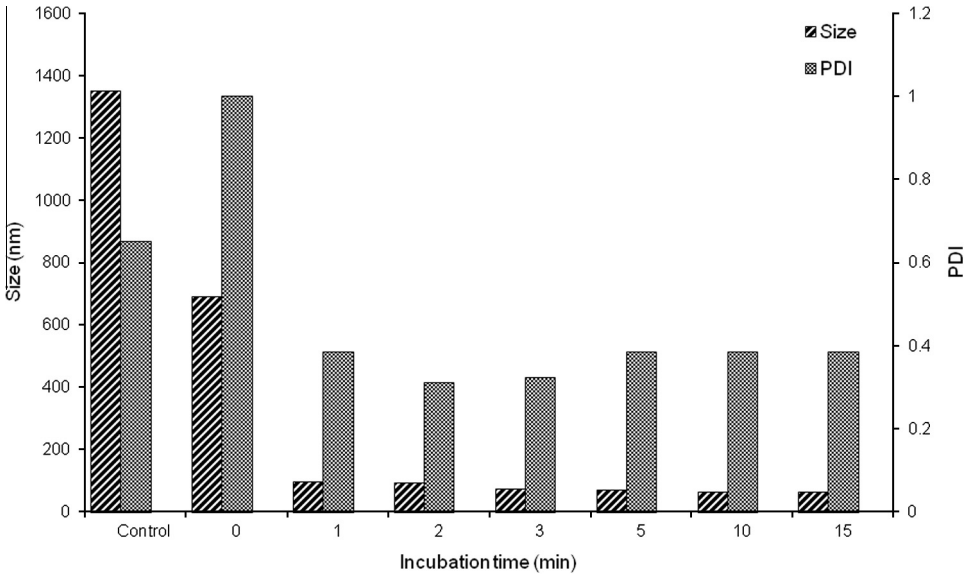

Fig. 1. Hydrodynamic diameter (*Z* value) of gold nanoparticles biosynthesized by *T. viride* at 30 °C at different time intervals and their respective poly dispersity index (PDI).

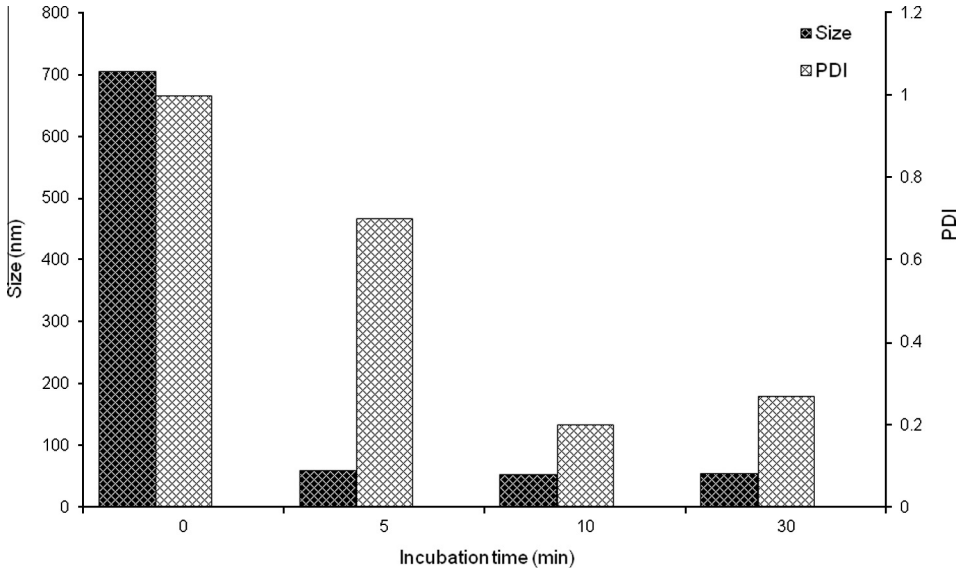

Fig. 2. Hydrodynamic diameter (*Z* value) of gold nanoparticles biosynthesized by *T. viride* at 100 °C at different time intervals and their respective poly dispersity index (PDI).

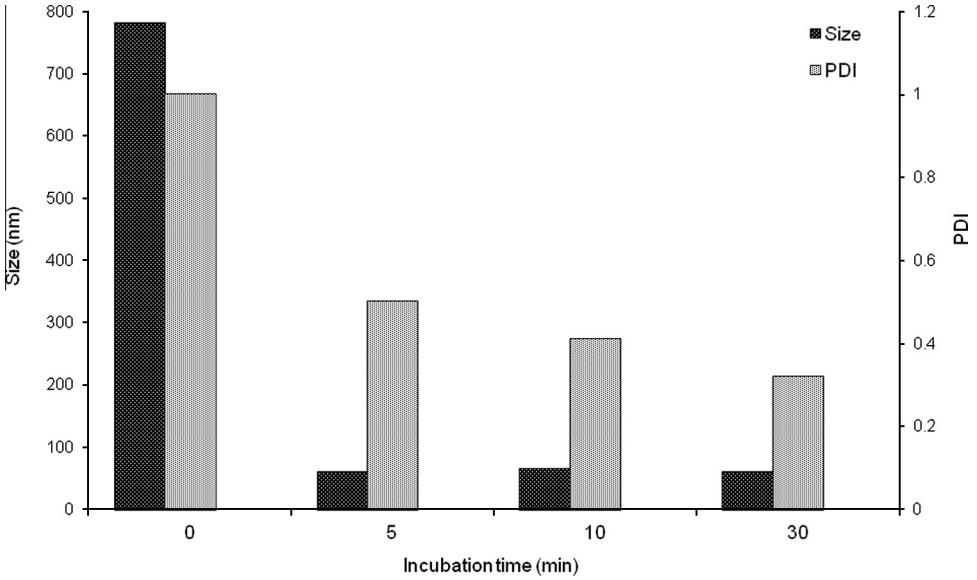

Fig. 3. Hydrodynamic diameter (*Z* value) of gold nanoparticles biosynthesized by *H. lixii* at 100 °C at different time intervals and their respective poly dispersity index (PDI).

3.3.5. Transmission electron microscopy (TEM)

To collect information about size and shape of gold nanoparticles, TEM measurement was carried out. Fig. S2 shows the TEM image obtained at different magnifications of 15,000×, 30,000× and 52,000× by the reaction of cell free extract and $HAuCl_4$ after 10 min of incubation time at 30 °C. A mixture of spheres, triangles, hexagons and rods were obtained (Fig. S2a and b) majority of which had spherical shape. TEM image taken at higher resolution (Fig. S2c) clearly demonstrated that the nanoparticles synthesized were well dispersed and scattered in nature. The gold nanoparticles must be stabilized by some agents in the extracellular secretions from the fungus *T. viride* which prevented the aggregation of gold nanoparticles. It is very clear from the TEM images that extracellular filtrate of *T. viride* is well capable of synthesizing nanoparticles as well as capping the particles so that their self aggregation is prevented. Previous studies on biosynthesis of gold nanoparticles also support the role of biomolecules as synthesizing as well as capping agents (Du et al., 2011). Further, crystalline nature of the synthesized particles were confirmed by SAED pattern.

TEM images taken after boiling the cell free extract yielded only spherical particles (Fig. S2d and e). The uniformity in shape can be attributed due to prevention of secondary growth of the gold nuclei at higher reaction temperature (Song et al., 2009).

Comparative histogram of gold nanoparticles synthesized at 30 °C and 100 °C (Fig. 4) reveals that while there is variation in size of gold nanoparticles synthesized at 30 °C, majority of the particles (60%) resided in range of 20–30 nm and few as bigger as 120 nm, most of the particles synthesized at 100 °C (82%) were below the range of 20 nm. The decreased size was maintained due to inhibition of the secondary reduction process of the nuclei at higher reaction rate. Similar trend had been observed with silver nanoparticles synthesized from plant extracts of *Diopyros kaki*, *Magnolia kobus* and *Pinus densiflora* (Song et al., 2009).

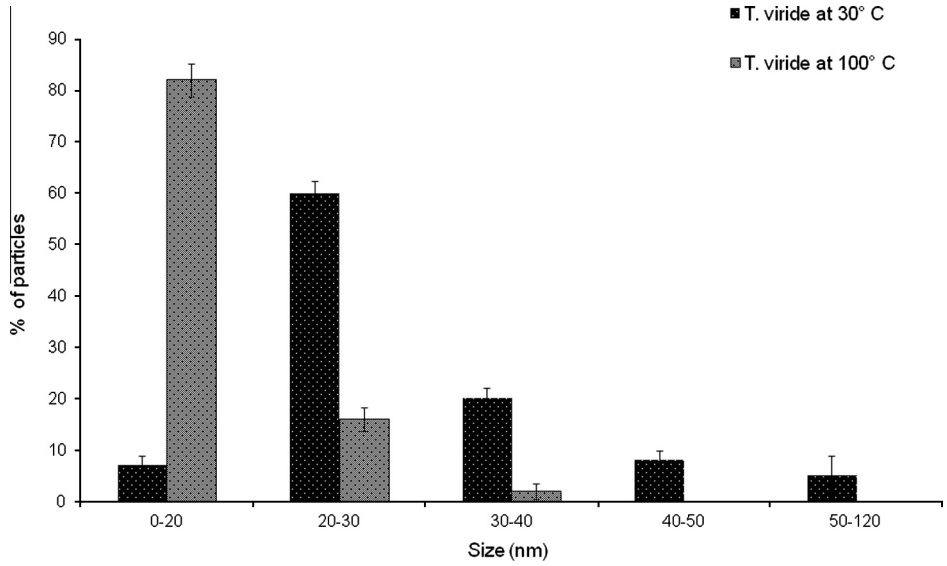

Fig. 4. Particle size distribution histogram and their percentage determined from TEM images at 30 °C and 100 °C by *T. viride*.

Two different patterns of nanotized particle were obtained by *H. lixii* at boiling temperature, first 74% of the population consisted of the particles below 20 nm and second was 19% population ranged between 20 and 30 nm. The particles were spherical in shape, similar with the results obtained from *T. viride*. This may happen due to incomplete prevention of secondary nucleation.

3.3.6. EDAX spectroscopy

A strong gold signal was obtained at 2 and 9.5 keV confirming the presence of gold. Strong signals of C, O, and P were also observed suggesting the role of biomolecules such as enzymes and secondary metabolites in synthesis and capping of gold nanoparticles (Shankar et al., 2004).

3.3.7. Effect of concentration of cell free extract of T. viride and H. lixii and substrate (Chlorauric acid)

Three different concentrations of cell free extract viz. 100%, 50%, and 10% were used to investigate the rapid synthesis of gold nanoparticles for both the fungal cell free extract. Though the synthesis took place in all the combinations, only 10% concentration of supernatant of *T. viride* was able to synthesize the nanoparticles rapidly where as the cell filtrate of *H. lixii* did not show any property of rapid reaction at room temperature. The 10% boiled extracts of both fungi were able to synthesize gold nanoparticles. Similarly among two concentrations of Chlorauric acid ($HAuCl_4$) were used for biosynthesis of gold nanoparticles (250 and 500 mg/l), only 250 mg/l yielded the gold nanoparticles, within 10 min.

3.3.8. Effect of pH

The ability of *T. viride* and *H. lixii* to synthesize gold nanoparticles was evaluated at pH 5, 7 and 9. Nanoparticles by cell free extract of *T. viride* were synthesized at pH 7 and 9 but not at pH 5, at room temperature. While *H. lixii* was unable to synthesize nanoparticles at room temperature. Because protonation of the carboxylic groups may occur at lower pH, the electrostatic interactions cannot impart stability to particles in solution (Bastús et al., 2011), resulting in either no synthesis or instability to the particles. Role of pH in biosynthesis of nanoparticles has also been demonstrated earlier (Sneha et al., 2011). Both reported the formation of large number of stable, uniform and spherical particles at higher temperature while at lower pH aggregation was observed. As the temperature was increased to 100 °C, the synthesis was observed in both the isolates at all the three pH. Increased activation energy as well as reducing power of the biological moieties at high temperature may be the cause of such rapid reduction irrespective of the pH (Sneha et al., 2011).

3.4. Antimicrobial activity of gold nanoparticles

3.4.1. Plate and broth assay

Antimicrobial activity of biosynthesized gold nanoparticles was assessed against human pathogens *E. coli*, *S. sonnei* and plant pathogen *P. syringae*. Dose dependent antimicrobial activity of biosynthesized gold nanoparticles was observed against all three pathogens. Fig. 5a–c shows the colony forming units (CFU) of the three pathogens in presence of biosynthesized gold nanoparticles in different concentration for seven days. In all the three cases, 25% of supplemented nanoparticles were capable to inhibit the growth up to 53%, 47%, and 55% for *E. coli*, *S. sonnei* and *P. syringae*, respectively (Fig. 5d). While the antimicrobial activity decreased slightly after 7 days of treatment in case of *E. coli* and *S. sonnei*, the percent inhibition in case of *P. syringae* remained the same (Fig. 5d). Our results are in agreement with previous findings proving gold nanoparticles a good antimicrobial agent (Bryaskova et al., 2011; Mei et al., 2014), with potential of its applications in biomedical and agriculture.

Although the exact mechanism of inhibitory action of gold nanoparticles has not been elucidated yet, many mechanisms have been proposed. Cui et al. (2012) proposed that bactericidal activity of gold nanoparticles might be due to collapse of membrane potential, inhibiting ATPase activities to decrease the ATP level and to inhibit the subunit of ribosome from binding tRNA. Unlike antibiotics, GNPs possess various mechanisms to kill bacteria, which becomes very difficult for a bacteria to acquire resistance against them. As gold nanoparticles do not possess a risk toward human health, they can easily be used as new generation of antimicrobial agent.

3.4.2. Gold nanoparticles immobilization on cloth and disk diffusion assay

The antimicrobial property of gold nanoparticles was assessed against *S. sonnei*. Fig. S3a shows the efficacy of gold nanoparticles immobilized with sterile water where as Fig. S3b shows the efficacy of the same after immobilization with PVP. As the

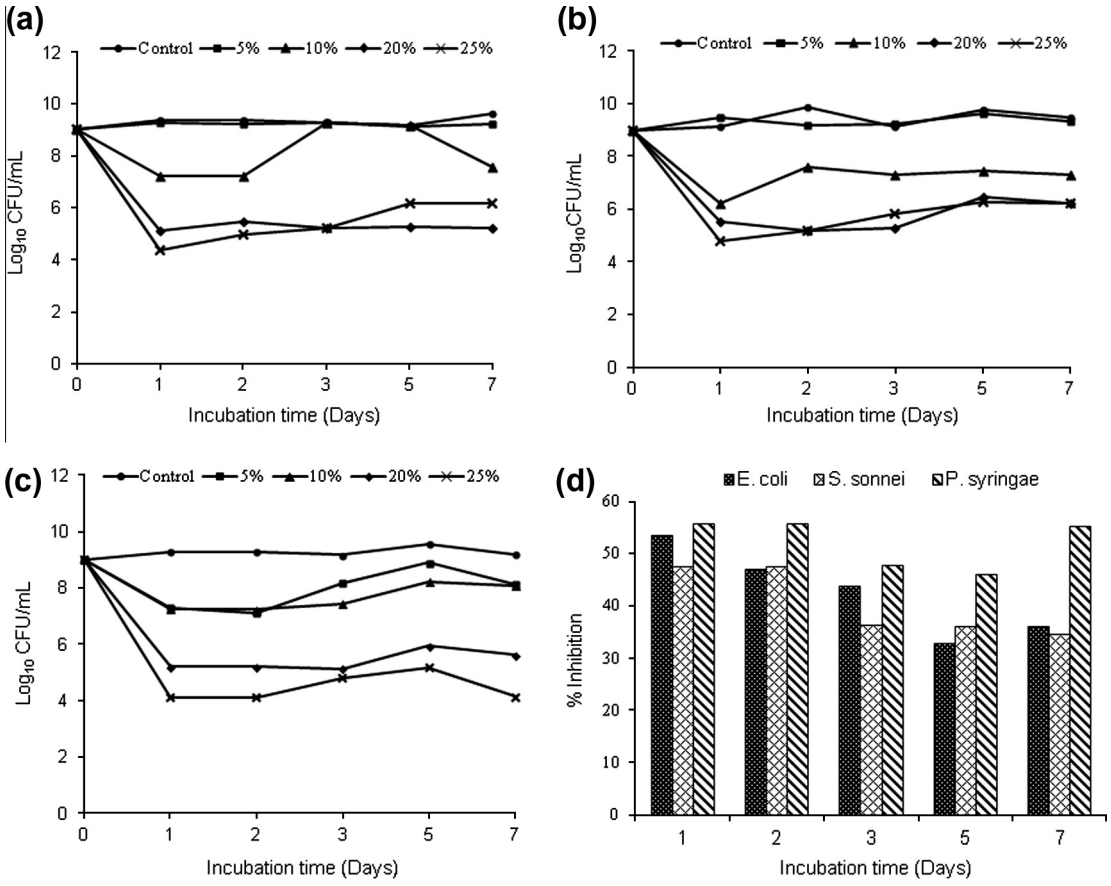

Fig. 5. Reduction in CFU count of (a) *E. coli*, (b) *S. sonnei* and (c) *P. syringae* after addition of 5%, 10%, 20%, and 25% of biosynthesized gold nanoparticles for a time period of seven days. (d) Percent inhibition of pathogenic bacteria after addition of 25% of gold nanoparticles to media over a time period of seven days.

concentration of the particles increased in both conditions, the inhibition zone on the plate increased consequently due to increase in toxicity. The cloth immobilized with PVP demonstrated higher antimicrobial activity as compared to the cloth immobilized with sterile water. The enhanced potential as antimicrobial agent of gold nanoparticles immobilized with PVP as compared with sterile water can be attributed due to prevention of agglomeration of particles and thus maintaining their antimicrobial activity (Bryaskova et al., 2011). As gold nanoparticles are reported to have no problems on human health (Cai et al., 2008), and as the biosynthesis is from non pathogenic fungi, they can be impregnated on contact lens, socks and bandages to avoid microbial contamination (Sathishkumar et al., 2010).

3.5. Catalytic activity of gold nanoparticles in 4-nitrophenol degradation

4-Nitrophenol was showing maximum absorbance at 400 nm due to formation of 4-nitrophenolate ions. Reason behind the formation of 4-nitrophenolate ions was the alkaline medium which was provided by $NaBH_4$. Despite of thermodynamic feasibility of both compounds, the reduction of 4-nitrophenol was not taking place due to large thermodynamic potential difference between 4-nitrophenol and $NaBH_4$ (Gangula et al., 2011). To initiate the reaction, a catalyst was required that was fulfilled by biocatalyst gold nanoparticles. This biocatalyst facilitated electron relay from the donor BH_4 to acceptor 4-nitrophenol to overcome large thermodynamic potential difference and reducing 4-nitrophenol to 4-aminophenol which can be qualitatively monitored by UV–vis spectroscopy.

In the absence of gold nanoparticles, the reaction failed to proceed further and imparted a yellow color even after several days. The color disappeared after 30 mins after the addition of 50 μl of biosynthesized gold nanoparticles. In accordance with the visual observations, the absorbance decreased from 400 nm to a new peak at 260 nm indicating formation of 4-aminophenol (Min et al., 2007).

Kinetic study of degradation of 4-nitrophenol and formation of 4-aminophenol was also monitored over a time period of 45 min. On addition of nanoparticles, the absorbance at 400 nm decreased continuously for 35 min and became constant thereafter. Similarly, absorbance at 260 nm increased till 30 min of addition of biosynthesized gold nanoparticles and became stable for rest of the period. Sinha et al. (2013) has also observed similar kinetic plot for degradation of nitrobenzene to aniline at 268 and 230 nm respectively. Gold nanoparticles used in this study can be reused as biocatalyst for further degradation of 4-nitrophenol as they can be procured back by centrifuging the reaction mixture at 5000 rpm for 5 min. The small quantity of gold nanoparticles required and its reuse for bioremediation purposes not only makes it a substitute for catalyst matrix (Srivastava et al., 2013) but also provides a new hope to green and low cost bioremediation.

4. Conclusions

An ecofriendly and rapid method of nanoparticles biosynthesis was developed by using biocontrol agents *T. viride* and *H. lixii*, which were able to overcome the limitations of physical and chemical methods of nanoparticles synthesis. There may be involvement of either secondary metabolites or, denatured proteins, as the fungi

were capable to synthesize the nanoparticles even at 100 °C. Quick biocatalytic conversion of 4-nitrophenol to 4-aminophenol by gold nanoparticles provides a new hope of green bioremediation where as the inhibition of pathogenic bacteria proves their candidature as a new generation antimicrobial agent.

Acknowledgements

The study was supported by New Initiative (as a Cross Flow Technology project) "Root Biology and Its Correlation to Sustainable Plant Development and Soil Fertility" (RootSF; BSC0204) from the Council of Scientific and Industrial Research (CSIR), New Delhi, India. M.K. would like to thank CSIR for providing her Senior Research Fellowship.

Appendix A. Supplementary data

Supplementary data associated with this article can be found, in the online version, at http://dx.doi.org/10.1016/j.biortech.2014.04.085.

References

Abdelhalim, M.A.K., Mady, M.M., Ghannam, M.M., 2012. Physical properties of different gold nanoparticles: ultraviolet–visible and fluorescence measurements. J. Nanomed. Nanotechnol. 3, 1–5.

Ahmad, A., Mukherjee, P., Senapati, S., Mandal, D., Khan, M.I., Kumar, R., Sastry, M., 2003. Extracellular biosynthesis of silver nanoparticles using the fungus *Fusarium oxysporum*. Colloids Surf. B 28, 313–318.

Ai, L., Jiang, J., 2013. Catalytic reduction of 4-nitrophenol by silver nanoparticles stabilized on environmentally benign macroscopic biopolymer hydrogel. Bioresour. Technol. 132, 374–377.

Bastús, N.G., Comenge, J., Puntes, V., 2011. Kinetically controlled seeded growth synthesis of citrate-stabilized gold nanoparticles of up to 200 nm: size focusing versus Ostwald ripening. Langmuir 27, 11098–11105.

Bryaskova, R., Pencheva, D., Nikolov, S., Kantardjiev, T., 2011. Synthesis and comparative study on the antimicrobial activity of hybrid materials based on silver nanoparticles (AgNps) stabilized by polyvinylpyrrolidone (PVP). J. Chem. Biol. 4, 185–191.

Burda, C., Chen, X., Narayanan, R., Sayed, M.E., 2005. Chemistry and properties of nanocrystals of different shapes. Chem. Rev. 105, 1025–1102.

Cai, W., Gao, T., Hong, H., Sun, J., 2008. Applications of gold nanoparticles in cancer nanotechnology. Nanotechnol. Sci. Appl. 1, 17–32.

Cui, Y., Zhao, Y., Tian, Y., Zhang, W., Lüa, X., Jiang, X., 2012. The molecular mechanism of action of bactericidal gold nanoparticles on *Escherichia coli*. Biomaterial 33 (7), 2327–2333.

Das, S.K., Khan, M.M.R., Guha, A.K., Das, A.R., Mandal, A.B., 2012. Silver-nano biohybride material: synthesis, characterization and application in water purification. Bioresour. Technol. 124, 495–499.

Du, L., Xian, L., Feng, J.X., 2011. Rapid extra-/intracellular biosynthesis of gold nanoparticles by the fungus *Penicillium* sp. J. Nanopart. Res. 13, 921–930.

Eustisa, S., El-Sayed, M.A., 2006. Why gold nanoparticles are more precious than pretty gold: noble metal surface plasmon resonance and its enhancement of the radiative and nonradiative properties of nanocrystals of different shapes. Chem. Soc. Rev. 35, 209–217.

Gan, P.P., Ng, H.S., Huang, Y., Li, S.F.Y., 2012. Green synthesis of gold nanoparticles using palm oil mill effluent (POME): a low-cost and eco-friendly viable approach. Bioresour. Technol. 103, 132–135.

Gangula, A., Podila, R.M.R., Karanam, L., Janardhana, C., Rao, A.M., 2011. Catalytic reduction of 4-nitrophenol using biogenic gold and silver nanoparticles derived from *Breynia rhamnoides*. Langmuir 27 (24), 15268–15274.

Haiss, W., Thanh, N.T.K., Aveyard, J., Fernig, D.G., 2007. Determination of size and concentration of gold nanoparticles from UV–vis spectra. Anal. Chem. 79, 4215–4221.

Heiligtag, F.J., Niederberger, M., 2013. The fascinating world of nanoparticles research. Mater. Today 16 (7/8), 262–271.

Kasthuri, J., Veerapandian, S., Rajendiran, N., 2009. Biological and synthesis of silver and gold nanoparticles using apiin as reducing agent. Colloids Surf. B 68 (1), 55–60.

Kaushik, N., Thakkar, M., Snehit, S., Mhatre, M.S., Rasesh, Y., Parikh, M.S., 2010. Biological synthesis of metallic nanoparticles. Nanomed. Nanotechnol. Biol. Med. 6 (2), 257–262.

Knöpfel, T., Akemann, W., 2010. Nanobiotechnology: remote control of cells. Nat. Nanotechnol. 5, 560–561.

Kuang, Y., Zhou, Y., Chen, Z., Megharaj, M., Naidu, R., 2013. Impact of Fe and Ni/Fe nanoparticles on biodegradation of phenol by the strain *Bacillus fusiformis* (BFN) at various pH values. Bioresour. Technol. 136, 588–594.

Kumar, P., Misra, A.K., Modi, D.R., Gupta, V.K., 2012. Biocontrol potential of *Trichoderma* species against mangomal formation pathogens. Arch. Phytopathol. Plant Prot. 45 (10), 1237–1245.

Mei, L., Zhang, X., Wang, Y., Lu, Z., Zhao, Y., Li, C., Zhang, W., Luo, Y., 2014. Multivalent polymer-Au nanocomposites with cationic surfaces displaying enhanced antimicrobial activity. Polym. Chem. http://dx.doi.org/10.1039/C3PY01578E.

Min, S., Risheng, Y., Yahua, Y., Shengsong, D., Wenxia, G., 2007. Degradation of 4-aminophenol by hydrogen peroxide oxidation using enzyme from *Serratia marcescens* as catalyst. Front. Environ. Sci. Eng. China 1 (1), 95–98.

Mishra, A., Nautiyal, C.S., 2009. Functional diversity of the microbial community in the rhizopshere of chickpea grown in diesel fuel-spiked soil amended with *Trichoderma ressei* using sole-carbon-source utilization profiles. World J. Microbiol. Biotechnol. 25, 1175–1180.

Mukherjee, P., Roy, M., Mandal, B.P., Choudhury, S., Tewari, R., Tyagi, A.K., Kale, S.P., 2012. Synthesis of uniform gold nanoparticles using non-pathogenic biocontrol agent: evolution of morphology from nano-spheres to triangular nanoprisms. J. Colloid Interface Sci. 367, 148–152.

Mullai, P., Yogeswari, M.K., Sridevi, K., 2013. Optimisation and enhancement of biohydrogen production using nickel nanoparticles – a novel approach. Bioresour. Technol. 141, 212–219.

Sathishkumar, M., Sneha, K., Yun, Y.S., 2010. Immobilization of silver nanoparticles synthesized using *Curcuma longa* tuber powder and extract on cotton cloth for bactericidal activity. Bioresour. Technol. 101, 7958–7965.

Shahverdi, A.R., Minaeian, S., Shahverdi, H.R., Jamalifar, H., Nohi, A.A., 2007. Rapid synthesis of silver nanoparticles using culture supernatants of Enterobacteria: a novel biological approach. Process Biochem. 42, 919–923.

Shankar, S.S., Rai, A., Ahmad, A., Sastry, M., 2004. Rapid synthesis of Au, Ag, and bimetallic Au core Ag shell nanoparticles using neem (*Azadirachta indica*) leaf broth. J. Colloid Interface Sci. 275, 496–502.

Sinha, A.K., Basu, M., Sarkar, S., Pradhan, M., Pal, T., 2013. Synthesis of gold nanochains via photoactivation technique and their catalytic applications. J. Colloid Interface Sci. 398 (15), 13–21.

Sneha, K., Sathishkumar, M., Lee, S.Y., Bae, M.A., Yun, Y.S., 2011. Biosynthesis of Au nanoparticles using cumin seed powder extract. J. Nanosci. Nanotechnol. 11 (2), 1811–1814.

Song, J.Y., Jang, H.K., Kim, B.S., 2009. Biological synthesis of gold nanoparticles using *Magnolia kobus* and *Diopyros kaki* leaf extracts. Process Biochem. 44, 1133–1138.

Srivastava, S.K., Yamada, R., Ogino, C., Kondo, A., 2013. Biogenic synthesis and characterization of gold nanoparticles by *Escherichia coli* K12 and its heterogeneous catalysis in degradation of 4-nitrophenol. Nanoscale Res. Lett. 8, 70–78.

Sujitha, M.V., Kannan, S., 2013. Green synthesis of gold nanoparticles using Citrus fruits (*Citrus limon*, *Citrus reticulata* and *Citrus sinensis*) aqueous extract and its characterization. Spectrochim. Acta A 102, 15–23.

Tanga, B.C., Dawsona, M., Laia, S.K., Wang, Y., Suk, J.S., Yang, M., Zeitlin, P., Boyle, M.P., Fu, J., Hanes, J., 2009. Biodegradable polymer nanoparticles that rapidly penetrate the human mucus barrier. Proc. Natl. Acad. Sci. U.S.A. 106 (46), 19268–19273.

Tripathi, P., Singh, P.C., Mishra, A., Chaudhry, V., Mishra, S., Tripathi, R.D., Nautiyal, C.S., 2013. *Trichoderma* inoculation ameliorates arsenic induced phytotoxic changes in gene expression and stem anatomy of chickpea (*Cicer arietinum*). Ecotoxicol. Environ. Saf. 89, 8–14.